Journal of Physics: Conference Series **2420** (2023) 012058 doi:10.1088/1742-6596/2420/1/012058

Space charge analysis for low energy photoinjector

M Carillo[1,4], M Behtouei[2], F Bosco[1,3,4], L Faillace[1,2], L Ficcadenti[4],A Fukasaway[3] L Giuliano[1,4], A Mostacci[1,4], M Migliorati[1,4], B Spataro[2], J Rosenzweig[3] and L Palumbo[1,4]

[1]Sapienza University of Rome, 00161 Rome, Italy
[2]INFN-LNF, 00044 Frascati, Italy
[3]UCLA, Los Angeles, 90095 California, USA
[4] INFN-Sez.Roma1, 00161 Roma, Italy

E-mail: martina.carillo@uniroma1.it

Abstract. Beam dynamics studies are performed in the context of a C-Band hybrid photo-injector project developed by a collaboration between UCLA/Sapienza/INFN-LNF/RadiaBeam [1, 2].These studies aim to explain beam behaviour through the beam-slice evolution, using analytical and numerical approaches. An understanding of the emittance oscillations is obtained starting from the slice analysis, which allows correlation of the position of the emittance minima with the slope of the slices in the transverse phase space (TPS). At the end, a significant reduction in the normalized emittance is obtained by varying the transverse shape of the beam while assuming a longitudinal Gaussian distribution. Indeed, the emittance growth due to nonlinear space-charge fields has been found to occur immediately after moment of the beam emission from the cathode, giving insight into the optimum laser profile needed for minimizing the emittance.

1. Introduction

In the new generation of high-brightness beams [3] a fundamental role is played by the achievement of emittance compensation [4, 5]. This scenario includes the design of the Hybrid C-band photo-injector and the in-depth study of the dynamics of its output beam [6]. To do this, different approaches are exploited, such as beam slice analysis and the analytical study of the phenomena under consideration, including space charge fields.

2. Beam slice analysis

Slice analysis has a key impact to understand beam dynamics and in the emittance compensation process. Starting from the definition of the beam rms emittance it is possible to separate four different components due to slice splitting [7]. In this analysis we will neglect the emittance terms due to the linear and non-linear contributions of the transverse offsets between the slices themselves because they give a negligible contribution to the total projected emittance [8].

The transverse rms emittance is defined starting from the second order moments according to the equation [9]:

$$\varepsilon_{rms}^2 = \sigma_x^2 \sigma_{p_x}^2 - \sigma_{x,px}^2. \quad (1)$$

Let us take a beam of N particles, divided into S slices, each one populated by a variable number of particles M_i. σ^2 moments can be written as function of sum of the slice second order

moments:

$$\sigma_x^2 = \langle x^2 \rangle = \sum_{i=1}^{S} \sum_{j=1}^{M_i} \frac{x_j^2}{N} = \sum_{i=1}^{S} \frac{M_i}{N} \langle x^2 \rangle_i = \sum_{i=1}^{S} \frac{M_i}{N} \sigma_{x,i}^2 \tag{2}$$

where $\langle\rangle$ defines an ensemble average, and in the same way:

$$\sigma_{p_x}^2 \equiv \sum_{i=1}^{S} \frac{M_i}{N} \sigma_{p_x,i}^2 \ , \ \sigma_{xp_x} \equiv \sum_{i=1}^{S} \frac{M_i}{N} \sigma_{xp_x,i} \tag{3}$$

By replacing equation (2), and (3) in to equation (1) the rms emittance becomes:

$$\varepsilon_{rms}^2 = \sum_{i=j} \left(\sigma_{x,i}^2 \sigma_{p_x,i}^2 - \sigma_{xp_x,i}^2 \right) + \sum_{i \neq j} \frac{M_i M_j}{N^2} \left(\sigma_{x,i}^2 \sigma_{p_x.j}^2 - \sigma_{xp_x,i} \sigma_{xp_x,j} \right) \tag{4}$$

where the first sum in the left-hand side is the emittance definition of $i-$th slice $\varepsilon_{rms_i}^2$, and the second one defines the correlated slices emittance expression, ε_{corr}^2. Since our goal is to optimize the emittance compensation process, a study on the double emittance oscillation at the gun exit [10] is performed. We assume, as initial conditions, the ones at the exit from the photoinjector and we study the evolution in a long drift.

Every single slice satisfies the envelope equation of a bunch in a free space, evolving under the effect of space charge force and emittance pressure, and each slice has different initial conditions $(\sigma_{0_i}, \sigma'_{0_i})$ but also different charge denisty λ_i and energy γ_i. The second order moment in equation (4) can be written as function in terms of of the envelope function σ and its derivative, with respect to the longitudinal position z, σ':$\sigma_x = \sigma$, $\sigma_{xp_x} = \sigma\gamma\sigma'$ and $\sigma_{p_x} = \gamma\sigma'$. Assuming for simplicity, that each slice is populated by the same number of particles $M = S/N$, the correlated emittance term can be written as:

$$\varepsilon_{corr}^2 = \frac{1}{2S^2} \sum_{i \neq j} (\sigma_i \gamma_j \sigma'_j - \sigma_j \gamma_i \sigma'_i)^2. \tag{5}$$

2.1. Floettmann model

In Floettmann emittance compensation analysis [11] using the slice model, it was demonstrated that to understand the emittance growth [12], it is well to know the orientation of the rms distribution in phase space, in addition to the slice size. For thin slice, the slope m of the distribution can be fitted by a straight line in the phase space: $m = \gamma\langle xx' \rangle / \langle x^2 \rangle$, where x and x' represent the phase space coordinates, and $\langle x \rangle = \langle x' \rangle = 0$ is assumed. It is possible to derive the derivative of the beam envelope as function of the slope parameter m. In fact by definition:

$$\sigma' = \frac{1}{2\sigma_x} \frac{\partial}{\partial z} \langle x^2 \rangle = \frac{\langle xx' \rangle}{\langle x^2 \rangle^{1/2}}, \tag{6}$$

so that,

$$m = \frac{\gamma \langle xx' \rangle}{\langle x^2 \rangle} = \frac{\gamma \sigma'}{\sigma}. \tag{7}$$

Thus the spread of m of all slices shrinks: the sizes of the slices and their speed of rotation evolve differently due to the difference in the space charge forces which they are subject to. Taking into account only two slices, the condition for obtaining a minimum of emittance is:

$$\Delta m = 0. \tag{8}$$

In Floettmann the analysis takes into account two beam slices, respectively with high and low perveance, and he proved equation (7), studying that the evolution of the slope m of the other slices with the intermediate perveance must be included in the interval of the two examined slices. In the two-slice case, the evolution equation is a second order equation, and hence the condition in equation (8) is reached in two positions. For this reason, two minima are observed in the emittance oscillation.

2.2. Multi-slice model

The goal is to explain why in a real physical beam, where the number of slices is greater than two, only two minima of emittance are still observed. For this reason the Floettmann analysis has been extended to a multi-slice model.

The relation in equation (7) is exploited by substituting it in the correlated emittance equation of the slices (equation (5)):

$$\varepsilon_{corr}^2 = \frac{1}{2S^2}\sum_{i\neq j}(\sigma_i m_j \sigma_j - \sigma_j m_i \sigma_i)^2 = \frac{1}{2S^2}\sum_{i\neq j}\sigma_i^2\sigma_j^2(m_i - m_j)^2. \tag{9}$$

The validity of this model is confirmed for two slice. As can been see from the multi-slice equation (9), it is not so easy to identify a condition on m in the multi-slice case. In fact, the squared slope difference in the phase space for each pair of beam slices is weighted by the product of their slice sizes. To show that, we applied this analysis to the case of the C-band hybrid photoinjector. The beam is split into 10 slices as described in [13], and evolves in a one meter drift long.

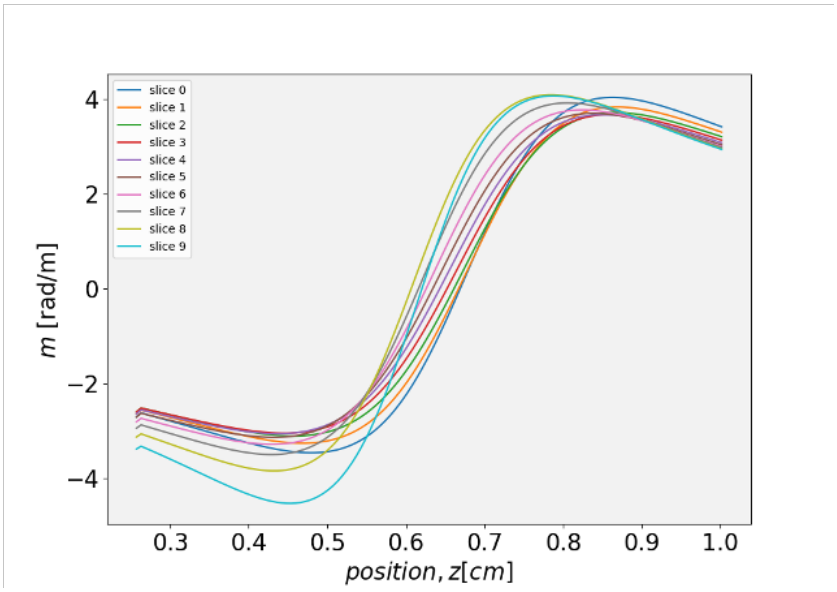

Figure 1. Evolution of the TPS slope m (equation (7)) as a function of the position in the drift. Each color represents one of the 10 slices the bunch has been divided into, where slice number 0 and 9 represents respectively the tail and the head slice.

Starting from the knowledge of the distributions in the TPS, the evolution of m for each slice along the drift is obtained using equation (7): the slices exiting from the photoinjector have a negative m value as they are still affected by the focusing effect of the solenoid. After reaching the minimum, the space charge forces dominate the focusing effects and the slices rotate in the opposite direction until they reach a positive defocusing slope.

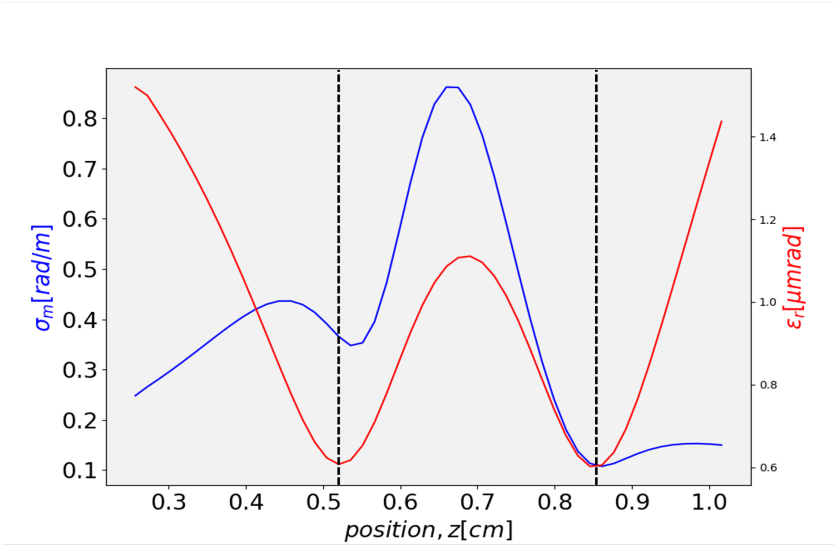

Figure 2. The slope spread σ_m of the TPS (blue curve) as a function of the drift position, in comparison with the rms emittance oscillation (red curve). The two vertical black dotted lines represent the exact position of the two emittance minima.

Whereas in the two-slices Floettman model the emittance minimum condition is reached when the slices are exactly overlapping (equation (8)), in the multi-slice model the minimum emittance conditions should occur when the difference of all the slopes of the slices m_i is minimal. For this reason the trend of the spread of m of the 10 beam slices along the drift has been studied and compared, in figure 2, with the emittance oscillation. What figure 2 shows is that, in the multi-slice case, the positions of the emittance minima do not coincide precisely with the positions for which the spread is the smallest one, but they remain in a close range. The reason for this behavior is implicit in equation (9). In fact it is not possible to extract a direct dependence on the spread σ_m, since the differences $|m_i - m_j|$ are weighted by the dimensions of the slices themselves, which change along the drift.

In any case, observing the slices evolution in the TPS, it is possible to obtain information on why only two minima of emittance occur even in the case with many slices. The slices leaving the photoinjector have a negative slope in the TPS (figure 1), which indicates their focusing behavior. Since they rotate with different speeds, they can reach a condition of maximum alignment with each other already in the focusing half-plane, and therefore identify the first emittance minimum. When, due to compression, the effect of space charge forces becomes dominant with respect to the effect of the focusing kick, the slices change direction of rotation in the phase space and assume a positive slope value. Also in this half-plane they will reach a second alignment condition, which determines the identification of the second emittance minimum. We could expect that continuing to have different speeds, the slices can re-align other times and therefore identify other positions of minimum emittance. What actually happens is that the slices now have a de-focusing behavior, and therefore their size tends to increase significantly. This means that even if they were re-aligned among themselves, the weight of the contribution of the size product in equation (9) would be so significant that the emittance value would still be high, and therefore not significant for the emittance compensation goal.

3. Space charge at the cathode

Beam shaping at the photocathode injection has been investigated with two different transverse laser distributions assumed with the aim of emittance compensation [2]. The first form is a simple uniform transverse distribution in r ("flat-top"), while the second one has the shape of a 1σ Cut-Gaussian. Indeed, using a uniform transverse laser illumination, the optimized rms normalized emittance has been found to be near 0.75 $mm-mrad$, while when one uses the truncated Gaussian laser profile on the photocathode, this normalized emittance decreases dramatically, to 0.46 $mm-mrad$. Slice analysis was used to explain the reason for this.

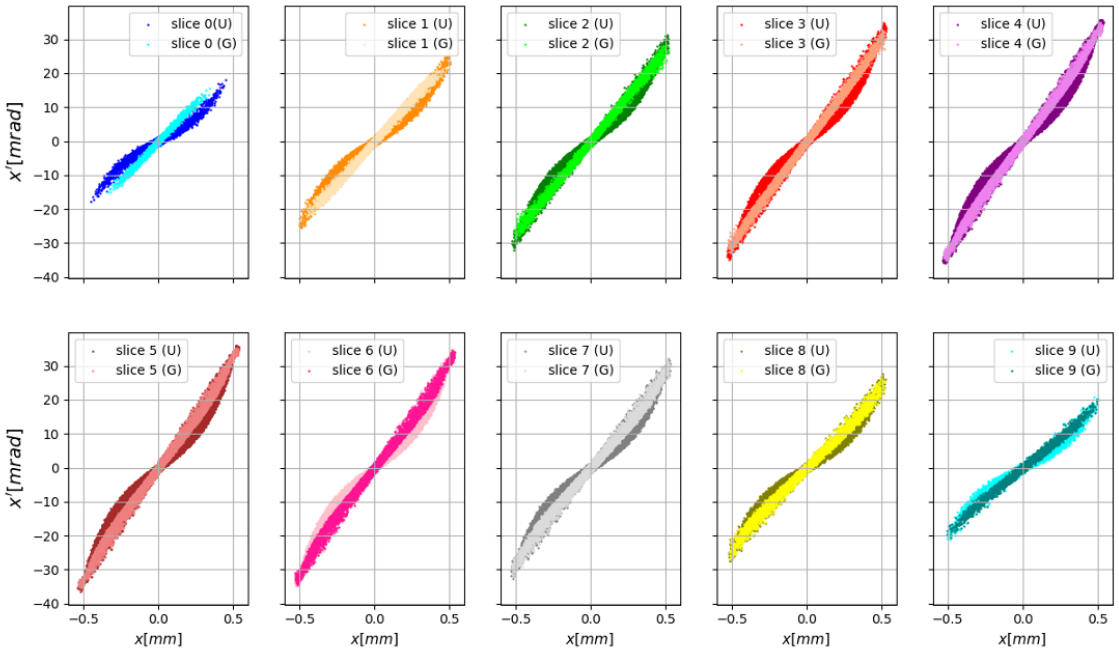

Figure 3. Slices comparison in the TPS for the beam just generated by the cathode. The two different colors in each plot represent the Cut-Gaussian and Flat-top distributions respectively, for each of the 10 slices.

Both beams are divided into 10 slices of equal length, and the TPS is analyzed. As shown in figure 3, it is evident that, by overlapping the same beam slices, the beam with the Cut-Gaussian distribution has a more linear trend than that of the Uniform case. This effect is visible already near of the photo-cathode, where the two distributions are generated. The reason is in the space charge forces expression [14].

Starting from the scalar potential solution of the not-homogeneous wave equation and using the Green function method [15], it is possible to obtain the radial space charge field expression as a function of the radial ($R(r)$) and longitudinal ($\lambda(z)$) distributions, for a fixed longitudinal position $\hat{z}$:

$$E_r^{(sc)}(r,\hat{z}) = -Q\int \frac{dk}{2\pi} e^{ik\hat{z}}\tilde{\lambda}(k)\frac{\partial \mathcal{S}(r,k)}{\partial r}, \tag{10}$$

where $\mathcal{S}$ represents the surface integral:

$$\mathcal{S}(r,k) = 2\pi\int_0^a \tilde{G}(r,r',k)R(r')r'dr', \tag{11}$$

and k is the wave vector in the Fourier space.

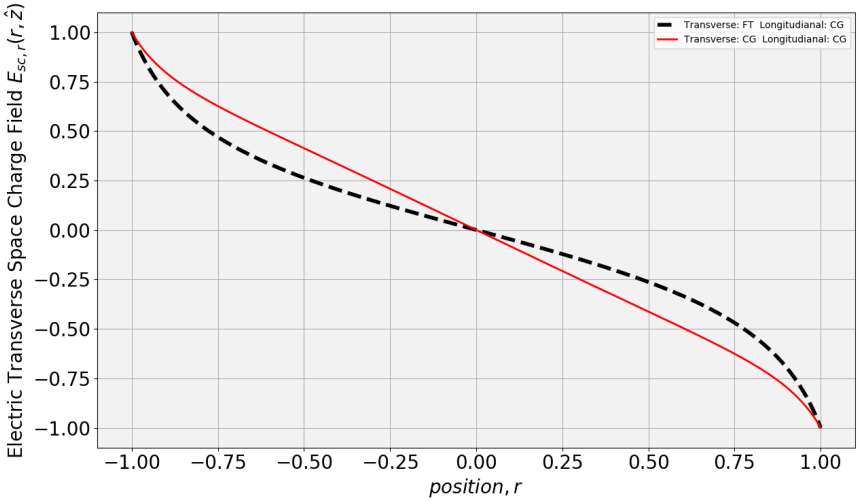

Figure 4. Normalized radial space charge field as a function of the normalized radial position. The field is compared with the same Gaussian longitudinal distribution while the transverse distributions varies from 1σ Cut-Gaussian (red curve) to Flat-Top (black dashed curve).

Plotting equation (10) for the two distributions, the behaviour in figure 4 is obtained. This shows that in the Cut-Gaussian case the space charge forces are more linear than in the Flat-Top case and, therefore, the contribution to the emittance is lower since the blow-out regime is reached earlier.

4. Conclusion and future goals

Several criteria for emittance compensation were analyzed using the slice analysis. In particular, the Floettmann model for the emittance oscillation has been extended to the multi-slice case, allowing the understanding of the presence of only two emittance minima, even in the multi-slice case.

Furthermore, a study on the dependence of the emittance on the laser distribution on the photocathode surface was performed, leading to derive the generic expression of the space charge fields for newly generated beams (equation (10)). The latter paved the way for a more complete study of the distributions used in the field of high-brightness accelerators, in order to reduce the beam emittance.

Acknowledgments

This work is supported by DARPA GRIT under contract no. 20204571 and partially by INFN National committee V through the ARYA project.

References

[1] Faillace L *et al.* 2021 *Proc. 12th Int. Particle Accelerator Conf. (IPAC'21)* (Campinas, Brazil) pp 2714–17
[2] Faillace L *et al.* 2022 *Phys. Rev. Accel. Beams* **25** 063401
[3] Rosenzweig J B *et al.* 2019 *Phys. Rev. Accel. Beams* **22** 023403
[4] Ferrario M *et al.* 2010 *Phys. Rev. Lett.* **104** 054801
[5] Rosenzweig J 2003 *Fundamentals of beam physics* (Oxford: Oxford University Press)
[6] Bosco F *et al.* 2021 *Proc. 12th Int. Particle Accelerator Conf. (IPAC'21)* (Campinas, Brazil) pp 3185–88
[7] Mitchell C 2015 A General Slice Moment Decomposition of RMS Beam Emittance *Preprint* ArXiv:1509.04765
[8] Niemczyk R 2021 *Subpicosecond-resolved emittance measurements of high-brightness electron beams with space charge effects at PITZ* Ph.D. thesis University of Hamburg

[9] Serafini L and Rosenzweig J B 1997 *Phys. Rev.* E **55** 7565
[10] Ferrario M *et al.* 2007 *Phys. Rev. Lett.* **99** 234801
[11] Floettmann K 2017 *Phys. Rev. Accel. Beams* **20** 013401
[12] Migliorati M *et al.* 2013 *Phys. Rev. Spec. Top. Accel Beams* **16** 011302
[13] Carillo M *et al.* 2021 *Proc. 12th Int. Particle Accelerator Conf. (IPAC'21)* (Campinas, Brazil) pp 3240–43
[14] Ferrario M, Migliorati M, and Palumbo L 2016 Space charge effects *Preprint* ArXiv:1601.05214
[15] Jackson J D 1998, *Classical Electrodynamics* (New York City:John Wiley and Sons)